Graph Based MRI Brain Scan Classification and Correlation Discovery

S. Seth Long and Lawrence B. Holder

Washington State University

Abstract—The shape of the human brain is correlated with many life events and psychological conditions. In this paper, we use a graph-based approach to represent the shape of the brain, including the shape of the ventricular system and shape relative to the skull. This graph representation is applied to classification of individuals based on level of cognitive impairment due to Alzheimer's Disease, level of education, and gender. The portions of the graph which are important to each distinction are found and visualized as an overlay on structural MR images. We find that whole-brain analysis in this manner allows automatic classification of images based on gender if the whole brain is included, but not strictly based on the ventricular system. Alzheimer's Disease is found to strongly affect ventricle shape, and education is found to correlate with the shape of the medial longitudinal fissure and the Sylvian fissure, which may be due to increases in overall brain mass due to education. Gender is predicted primarily by information in the MRI regarding facial structure and head shape. Finally, age is found to be easier to classify than any of the above distinctions. The classifier is found to have 90.9% accuracy differentiating scans of individuals 40 and younger from those from individuals 60 or older.

I. INTRODUCTION

Since the advent of brain imaging in the past half-century, many correlations have been discovered between brain shape and life events. For example, Maguire et al. found significant structural changes in the hippocampi of taxi drivers [1]. Further, Maguire et. al. determined that these structural changes were not the result of innate navigational ability, but rather acquired through use. In another example, Elsayed et al. [2] found correlations between the shape of the corpus callosum and musical ability. Elsayed et. al. were able to differentiate scans of brains from musicians and non-musicians, with up to 95% accuracy. Yet another example, by Nosarti et. al. [3] correlates ventricular size, hippocampus size, overall brain size, and other measures to premature birth, with the finding that a number of gray matter structures are reduced in size at adolescence in children born pre-term. All of these indicate strong correlations between brain structure and life events.

Diseases can also affect brain shape. For example, Alzheimer's Disease is known to cause a decrease in hippocampus size [4], as well as an increase in the size of the ventricles [5]. Early detection of Alzheimer's Disease may be possible using brain structure as an indicator [5].

Discovering these correlations can be done manually, however an automatic process may be able to replace human labor. In this paper, we focus on three areas: level of impairment due to Alzheimer's Disease, level of education, and gender. MR images including information about these classifications is available from the Open Access Structural Imaging Series [6]. We represent the shape of the brain as a tree. Branches correlating with the desired classification are found and used to form a feature vector, which can then be classified using a support vector machine. Our system can determine level of education (0 years or ≥ 4 years) with 81.7% accuracy, gender with 81.2% accuracy, and level of Alzheimer's Disease with 80% accuracy (70% when controlling for age in the healthy population). It can also determine age ≤ 40 or ≥ 60 in a balanced dataset of 93 young and 93 old individuals free of cognitive impairment with 90.9% accuracy.

Classification accuracy is an indication that the discovered correlations are correct, but does not directly provide information about brain structure. Besides classification, some machine learning systems provide a useful description of the criteria used for classification. For example, Subdue [7] provides the most discriminating subgraph, determined by high prevalence in one class and low prevalence in the other.

Instead of a single subgraph, our system uses a large number of discriminating branches, which may be visualized by highlighting the area of the MR image represented by each of the branches, and viewing 2D slices of the MRI in which the highlighting appears. Finding branches which are discriminating in the training set does not guarantee that these branches are also relevant to the classification in general. The likelihood that a branch is relevant in general increases if, having been found in the training set, it is also discriminating in the test set. This likelihood increases further if the branch is discovered in multiple folds of cross-validation. Using the idea of cross-validation to determine a set of branches which are likely to be relevant to the classification in general provides an idea of what the ideal classification hypothesis would be, and highlights areas which differentiate one class from the other. Results of this process are shown overlaied on 2D images of the brain. Alzheimer's Disease is shown to correlate with changes in the ventricular system, aging is shown to correlate with many changes throughout the brain, level of education is shown to correlate with many areas with concentrations in the medial longitudinal fissure and Sylvian fissures, and the accuracy on gender classification is revealed to be based on head shape and facial features.

II. PREVIOUS WORK

Some previous work has been focused on the particular problem of automatic recognition of Alzheimer's Disease from MRI data. For example, Klöppel et al. [8] consider each voxel

to be a feature in a feature vector, and then use a support vector machine to classify the resulting feature vectors. Cuingnet et al. [9] discuss and compare 10 different methods using a large dataset from 509 participants. As such, the study of automatic detection of Alzheimer's Disease is well-studied. In contrast, our study of classification of Alzheimer's Disease is used to validate a general-purpose classifier, which is then applied to level of education and gender, and can be applied to other measures as well in the future. Although the system can be used to classify scans depending on level of cognitive impairment, the focus of this work is automatic discovery of correlations in general rather than Alzheimer's disease classification.

The method by Klöppel et al. [8] differentiates discriminating vs. non-discriminating voxels, somewhat like the discriminating branches we propose below. However, a discriminating branch may represent a variable number of voxels depending on the length of the branch, and never represents as few as one voxel.

Elsayed et al. [2] have used graph-based shape representation to classify MR images using the 2D shape of the corpus callosum as it appears in a midsaggital section. Images were classified as either from a musician, or a non-musician, with up to 95% accuracy. Shape analysis was done by recursively subdividing the image into 4 quadrants to form a quadtree, terminating a branch if the area to be subdivided was sufficiently uniform in color. These trees were then classified by a frequent sub-tree classification method. This current work also represents shape using a tree of subdivisions.

Our previous work in this area [10] focused specifically on the ventricular system, although classification methods are similar. Also, no attempt was made previously to determine which brain areas were found to be useful for classification, merely that classification was possible using the methods presented.

III. Publicly Available MRI Data

Data is available from the Open Access Structural Imaging Series (OASIS) project [6]. This is a dataset consisting of over 400 structural MR images, some of individuals with varying levels of cognitive impairment. They are labeled according to the degree of cognitive impairment due to Alzheimer's disease. The data is in the Mayo Clinic Analyze 7.5 format [1]. The Nipy library can be used to access this data from Python code [11].

IV. Graph Representation

Prior to determining the graph representation of an image, the image is trimmed such that the edges of the image touch the skull, making centering consistent from one image to the next. This process was done automatically by moving each edge inward one voxel at a time until substantial light content was found, and then terminating the procedure. This bounding box is used as a means to consistently address location inside the brain, in a manner somewhat similar to the "anchor points" described by Megalooikonomou et al. in [12].

[1] http://www.grahamwideman.com/gw/brain/analyze/formatdoc.htm

The method of representing shape as a graph is described in detail in [10]. In brief, the area to be represented is recursively subdivided into 8 evenly-sized boxes. Subdivision is terminated when the color of a box is sufficiently homogeneous. These subdivisions form a tree, with each node representing either a subdivision or a box which will not be subdivided further. The maximum depth of the tree is limited in order to limit the computational time required for analysis. Leaves in the tree always correspond to boxes which are not further subdivided, either due to homogeneous color or depth limitation. Nodes are labeled to indicate a subdivision, or the reason for a formed leaf (light even color, dark even color, depth limitation). Edges are labeled in order to indicate which part of 3D space the division corresponds to, making each subdivision and leaf locatable in an MR Image. This representation was sufficient for classification of level of cognitive impairment and level of education when applied only to the ventricular system. Unlike the method in [10], there are no graphs which cannot be processed due to difficulty discovering particular structures.

When used for whole-brain analysis, a leaf at depth level 5 is (in voxels) approximately 5*7*7, for an area of 245 voxels. At depth 6, approximately 2.5*3.5*3.5, for an area of 16 voxels, although it should be noted that our technique will use whole voxels only, and so the decimal numbers are averages rather than common amounts. The size in voxels varies due to scale and head size variations from one image to the next. Most of the experiments described in this paper use a maximum depth of 5. Experiments with a depth of 6, did not improve accuracy, however the computational requirements of the task fully occupied a 296-processor cluster for several days on a 60-image dataset. An attempt to process a larger 100-image dataset was abandoned after two weeks. Generation of the trees themselves takes about a day using four threads on an Intel Q6600 quad-core processor.

V. Graph classification

Frequent Subgraph Classification involves finding a subgraph or set of subgraphs which are present in one class, but not the other. In this particular case, the graphs to be classified are trees. This allows for fast isomorphism testing to see if a particular branch is in a particular tree, and is used to calculate how many times a branch is present in the positive and negative examples. Using only a single leaf per discriminating branch, all possible discriminating branches can be enumerated in linear time relative to the number of nodes in the tree. The difference in prevalence of a branch between positive and negative sets is used to calculate a score indicating suitability of a branch for classification purposes. Branches which are found to be useful for discriminating between classes are used for classification. A tree is represented by a feature vector, where each feature corresponds to a discriminating branch, and indicates whether or not that particular branch is present in the tree. These feature vectors are then classified by support vector machine. We the libsvm [13] implementation. Details including distribution of the process over a computing cluster are given in [10].

VI. Discovering Correlations using Discriminating Branches

Cross-validation has been shown to be an effective method of evaluating the accuracy of machine-learning algorithms [14]. In order to find a set of branches which are most representative of the difference between classes, we apply a similar idea to branch selection. The dataset is divided into 10 test and 10 training sets as in 10-cross validation. In each fold, the 500 most discriminating branches from the training set are evaluated on the test set, and branches which are also discriminating on the test set are preserved. After all 10 folds have finished, branches appearing in the results of 5 or more folds are considered to be representative of a difference between the two classes under consideration. This process requires computational time comparable to the classification tests.

A limitation of this technique is that it does not allow an exact visualization of the classification hypothesis. The discriminating branches are used to generate features for a support vector machine, which may use them in any combination. The contribution of the SVM to classification is not recognized when discriminating branches are selected as above. This will prevent display of any conjunctive hypothesis consisting of multiple branches. However, by evaluating each branch individually on the test set, the result may be more representative of the differences between classes, even though it may not accurately represent the criteria used for classification.

Because branches are eliminated which are not found to be discriminating on the test set, higher classification accuracy is expected to be accompanied by a larger set of branches which were discriminating on the test set. This in turn produces a larger set of results. Also, lack of consistency between folds may indicate that the hypothesis used for classification, while it may have resulted in reasonable accuracy on the particular data on which it was evaluated, does not apply to the classification in general. Conversely, if a discriminating branch is found in many folds, it is likely to be relevant to the classification in general. Quantifying this tendency is left to future work, however it is noted in the results sections.

Once found, the area represented by the leaf of each discriminating branch is marked on sections of the MRI Image that contain area represented by that leaf. Because the leafs represent area from a 3D image, not all boxes appear on every 2D slice.

VII. Results and Discussion

All results were computed on a computing cluster at WSU. The cluster consists of 296 Intel Xenon processors arranged in nodes of 8 or 16 processors each. Processor frequency is not consistent throughout the cluster, most nodes are between 2.0 and 2.4 ghz. The algorithm for discriminating branch discovery is implemented using a custom map/reduce framework which enables operation on clusters using Portable Batch System to schedule jobs.

Maximum tree depth is fixed to 5 except as noted. In all cases, no more than 500 discriminating branches were allowed for any one fold of classification, to limit SVM overhead.

A. Alzheimer's Disease

Using a dataset of 60 individuals, 30 with CDR ≥ 1.0 and 30 healthy individuals, the system obtains an accuracy of 80%. However, this accuracy is reduced when controlling for the age of individuals. The youngest person in the OASIS dataset with cognitive impairment is 62, and the youngest healthy individual is 18. Using a dataset of 30 individuals with CDR ≥ 1.0 and 30 healthy individuals of at least age 62, the accuracy is reduced to 70%. This indicates that the system is able to find a correlation which is due to Alzheimer's Disease rather than age. The 80% accuracy without age control is up from 79.33 when classification is based on the third and lateral ventricles alone [10]. Processing on this 60-example dataset finishes in less than half an hour.

Including individuals with CDR 0.5, the system is unable to perform classification when healthy individuals under 62 are excluded. If individuals are randomly selected to form the healthy population without controlling for age, the system obtains an accuracy of 77.18%, up from 74.2% when using the ventricular system alone [10]. This indicates some ability to find correlation with age is present, even though the system can only distinguish cognitive impairment from age once it reaches CDR 1.0. This dataset includes a total of 198 examples, and requires a few hours to process depending on cluster load.

To test accuracy based on age alone, a dataset was constructed of 93 healthy individuals under age 40, and 93 healthy individuals over age 60, resulting in overall accuracy of 90.9%. Given this result, brain shape changes related to aging appear easier to detect than changes related to Alzheimer's Disease.

The branches represent locations dispersed through 3D space, and showing all of them on a single 2D slice is not possible. Figure 1 shows a representative sample. Most of the branches shown represent a location in the ventricular system, confirming that the ventricular system is strongly affected by this disease. This is consistent with findings such as [5] describing correlations between ventricular enlargement and progression of Alzheimer's disease. Note that some of the locations of importance change in content between the CDR 1.0 individual and the healthy individual. The boxes represent 3D space, and so in some cases a content of a box may change between images, but the change may not be apparent on the particular 2D section shown. Most of the ventricular system is inferior to the horizontal section from figure 1, and so boxes which extend downward to this area may include areas of CSF.

Accuracy on the dataset of CDR ≥ 1.0 vs. CDR 0 without age control was decreased to 78.33% when the trees were expanded to a maximum of 6 levels deep. This may be due to overfitting, assigning undue importance to exact details in the training set which are not upheld in the test set. It may also have been due to the number of discriminating branches discovered and discarded. On most experiments with a maximum depth of 5, no more than 1,000 discriminating branches were discovered per fold, whereas on the level 6 experiment generated approximately 7,000 branches per fold.

Most discriminating branches were found in at least one fold. Specific counts were:

1: 27
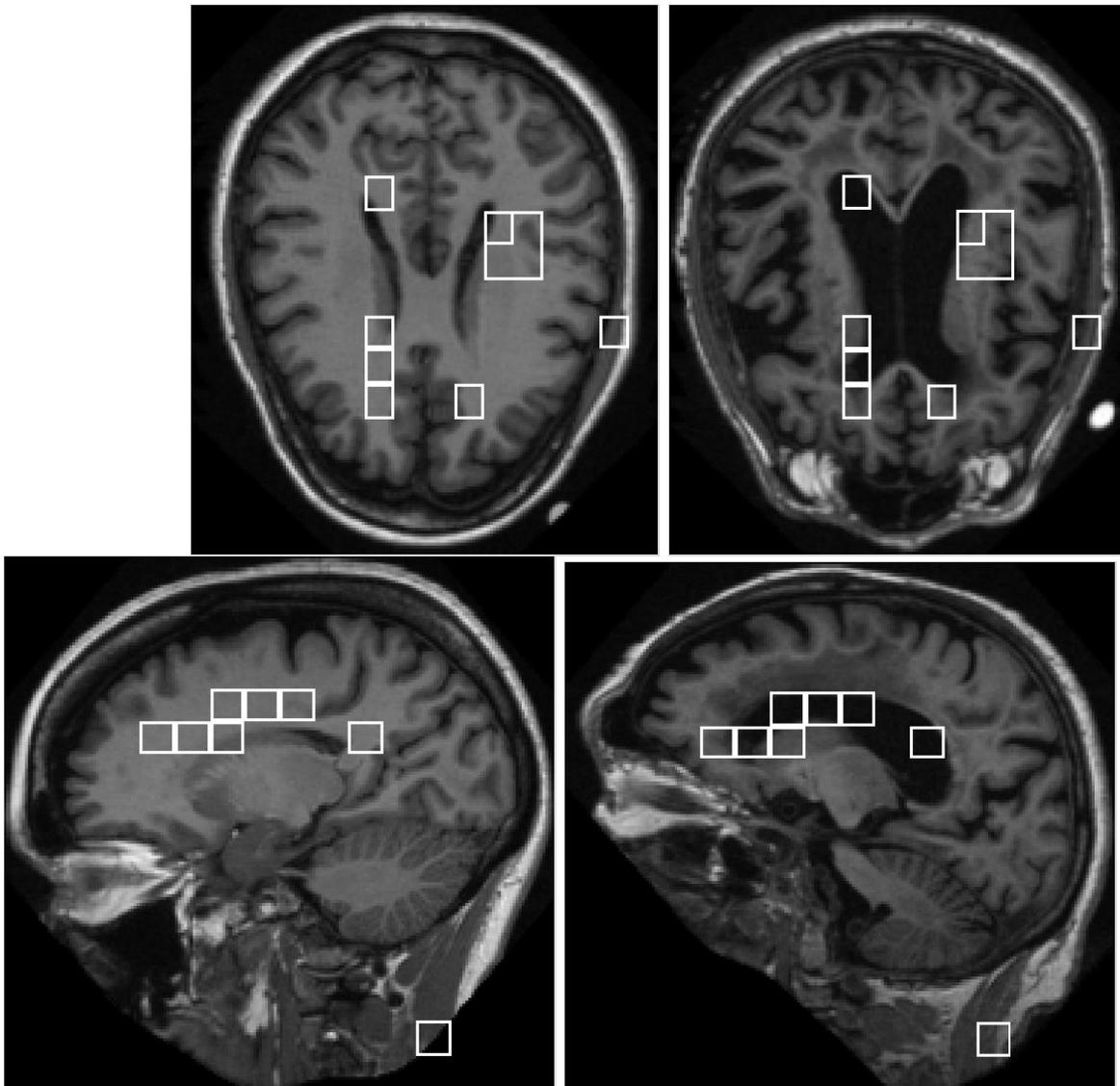
Fig. 1. Counterclockwise from upper left: (a) Horizontal section of the brain showing areas represented by discriminating branches found in at least 5 folds. The larger box on the right of the image indicates a branch which is shorter than the maximum allowed depth. (b) Same as a, except in an individual with CDR 1.0. (c) Saggital section offset laterally from the center showing the same in a healthy individual. (d) Same as c, except in an individual with CDR 1.0.

2: 304
3: 49
4: 29
5: 15
6: 9
7: 5
8: 4
9: 2

Although this does show commonality between folds, greater commonality is shown on other datasets (education, gender, age). This may reflect the lower accuracy on the Alzheimer's dataset compared to the others. No branches were common to all 10 folds. Using the dataset of individuals below 40 and over 60 (with no cognitive impairment), higher counts are obtained:

1: 29
2: 276

3: 97
4: 42
5: 42
6: 18
7: 36
8: 28
9: 23
10: 10

These higher counts indicate a more consistent set of discriminating branches in the age dataset compared to the Alzheimer's dataset. Figure 2 shows areas represented by discriminating branches. Areas important to age classification in some cases overlap with those for Alzheimer's classification, with many areas around the ventricular system. However, for age classification areas are more widespread, ranging throughout the cortex, and many areas found to be discriminating for Alzheimer's disease are not duplicated in
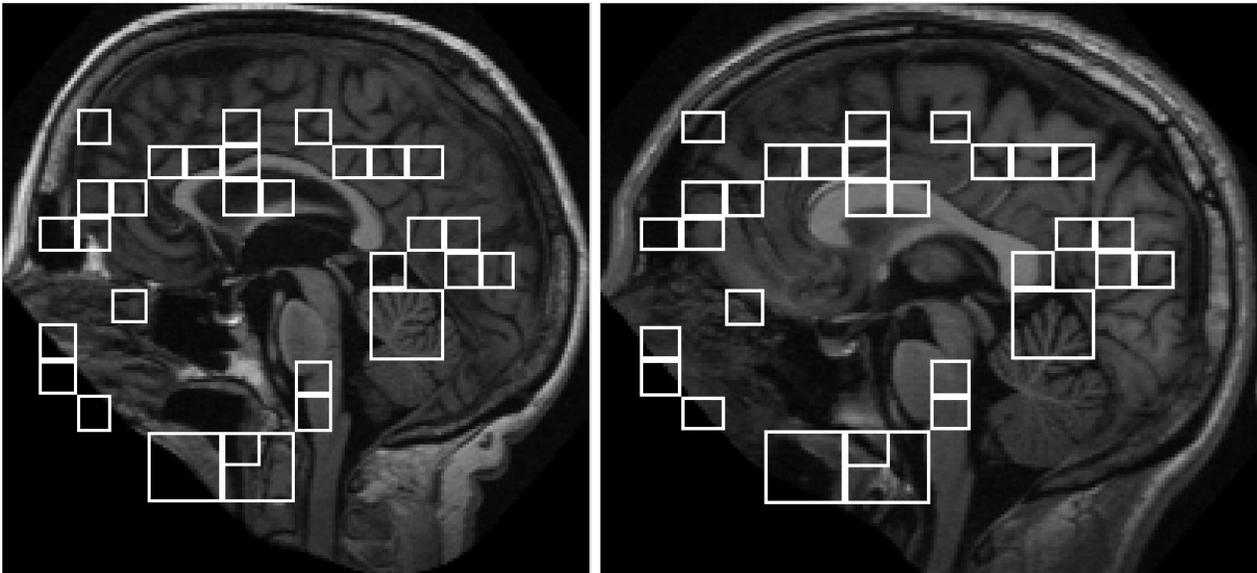
Fig. 2. Discriminating branch locations from the age dataset. Shown on a 74-year old brain (left) and a 21 year old brain (right). The differing width of the pictures is not due to image scaling, but rather reflects the differing shape of the area remaining after cropping out the parts of the MRI which do not contain tissue.
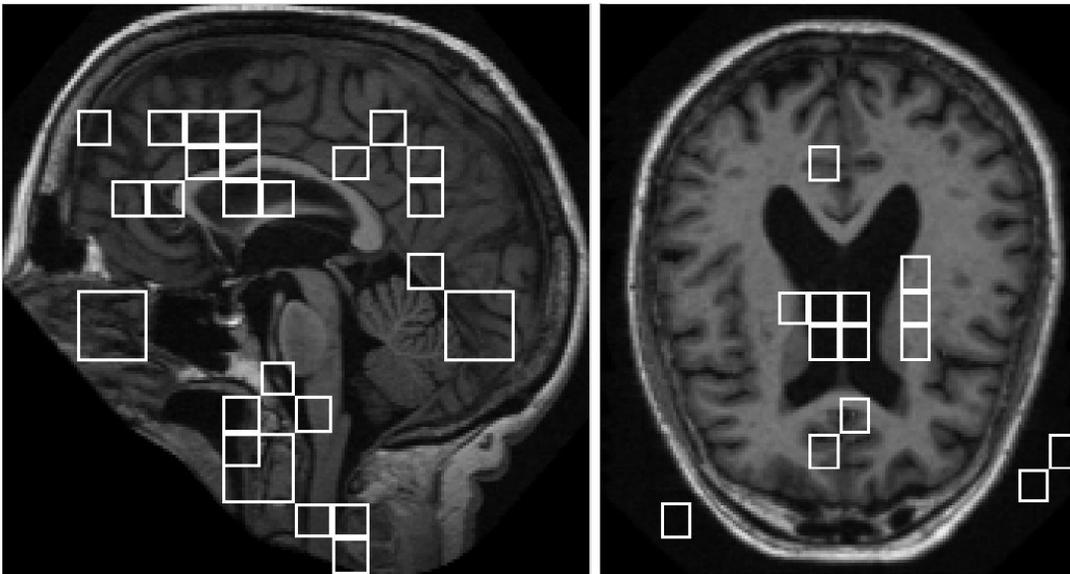
Fig. 3. Midsaggital and horizontal views showing discriminating branches from the education dataset. Note the large number of discriminating branches describing areas in the medial longitudinal fissure.

the aging result. Because the system was able to differentiate impaired individuals from healthy individuals even when age is controlled, it is expected that the classification criteria will differ.

In the OASIS dataset, all cognitively-impaired participants had at least a year of higher education. Alley et al. [15] found that greater education results in higher performance on intelligence tests in old age, and that verbal memory performance declined faster on well-educated participants. Wilson et al. [16] observed that highly-educated participants showed an increased rate of cognitive decline due to Alzheimer's disease. Given this, there may be some effect due to the level of education of the OASIS dataset participants. The sample

size of participants showing impairment is also small. 28 participants in the OASIS dataset exhibit CDR 1.0, and only 2 exhibit CDR 2.0.

B. Education

Using a dataset of 198 individuals, 99 of which have 4 or 5 years of education and 99 of which have 0, we obtain a classification accuracy of 81.7%, up from 77.9% when considering only the ventricular system [10]. This dataset is constructed from the OASIS dataset by random selection, and does not exclude individuals based on cognitive status or age. Balancing groups by age or cognitive impairment level could affect results. Figure 3 shows some discriminating branch
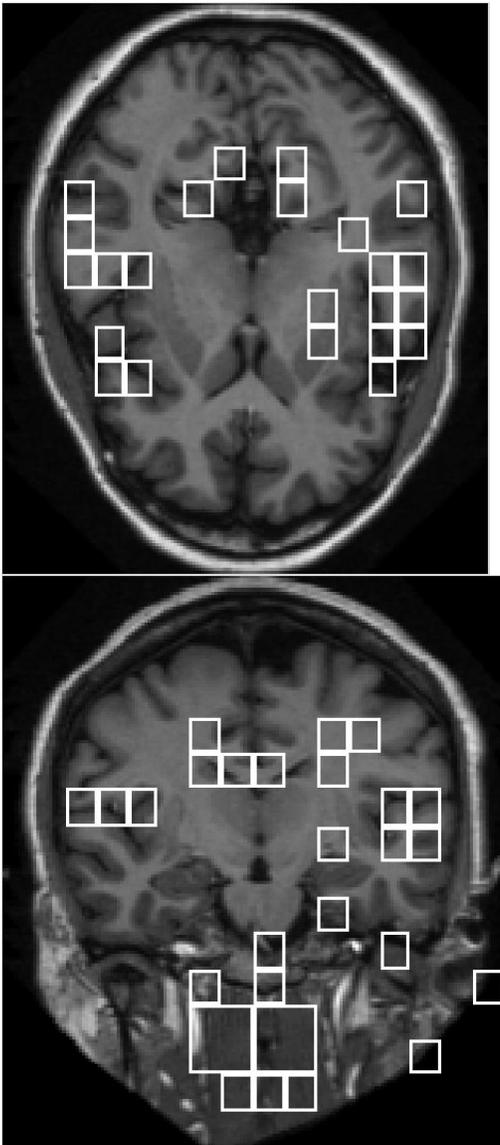
Fig. 4. Horizontal and coronal views from the education dataset showing highlighted areas in the Sylvian fissure.

locations from the education dataset. Overall effect appears to be widespread, with many diverse locations considered to be useful for classification. Many more branches were discovered by more than 5 folds compared with the Alzheimer's dataset. Specific counts were:

  1: 23
  2: 305
  3: 72
  4: 35
  5: 54
  6: 18
  7: 19
  8: 10
  9: 11
10: 1

Education is known to affect the aging brain. Coffey et al. [17] found a correlation between brain size and education in

elderly participants, of which there are many in the OASIS dataset. Correlations have also been found in non-elderly participants, for example, the hippocampus enlargement in taxi drivers found by Meguire et al. [1].

Figure 4 shows correlations discovered in the area of the lateral fissure on the education dataset. It is possible that correlations here are due to brain mass differences changing the amount of CSF in the lateral fissure. The same correlations are present in the age dataset to a lesser extent, and not at all in the Alzheimer's dataset. In addition, a large number of correlations appear in the medial longitudinal fissure, as seen in the midsaggital section in figure 3. Moving laterally away from the medial longitudinal fissure sharply decreases the number of correlating areas found.

It is worth noting that the system cannot tell differences in brain size except as related to skull size (that is, it does not use any measure of overall head size). However, the system can utilize the amount of cranial CSF by finding discriminating branches representing the area between the skull and gray matter. Figure 3 shows some discriminating branches in the cranial CSF, but the majority describe locations in the cortex. A few describe locations outside the skull, which presumably change relative to head shape.

Despite the branch selection procedure outlined above, branches are only guaranteed to be present in greater quantity in one class than the other in the data provided, not to have any biological significance. As such, results are a piece of evidence about correlations only, and concluding that head shape is related to education would require further evidence beyond that provided in figure 3.

C. Gender

Using a dataset of 308 individuals, 154 male and 154 female, the system is capable of 81.2% accuracy. Processing time is less than 6 hours. Using only the ventricular system, it was not possible to classify MR images based on gender [10]. Figure 5 shows locations represented by discriminating branches. Most of these are outside the ventricular system, and in fact many are outside the skull itself on the example shown in figure 5. Further areas are located in the facial regions. In the coronal section in figure 5, a concentration of branches is found on the lower right of the image. These appear to represent some sort of facial feature. Because the images could not be classified correctly using only the ventricular system, it is not surprising that no discriminating branches are apparent in that region.

Consistency between folds was higher on this dataset than any other. Specific counts were:

  1: 24
  2: 322
  3: 102
  4: 63
  5: 36
  6: 25
  7: 24
  8: 27
  9: 16
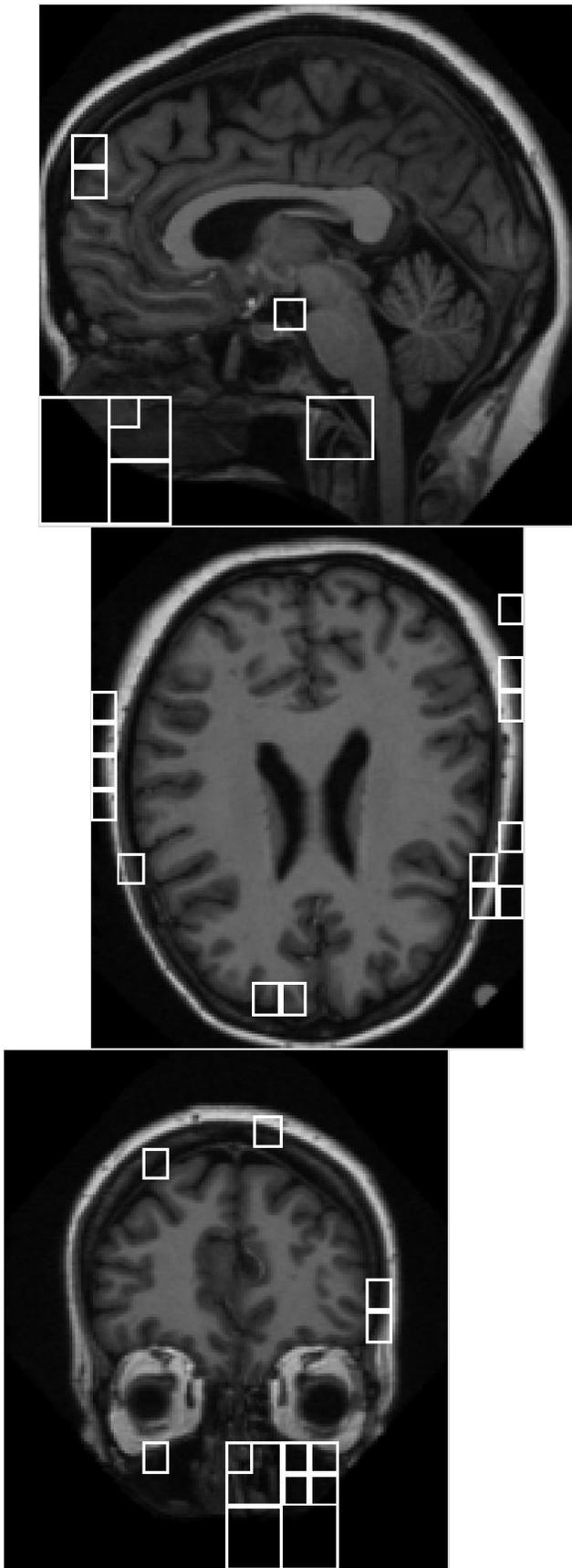
Fig. 5. From top, Midsaggital, horizontal, and coronal sections showing discriminating branch locations for gender determination.

10: 14

The brain is known to differ in structure between males and females [18]. Also, brain changes happen differently throughout life between the two genders [19], which may affect the OASIS dataset considering the large number of elderly participants. However, in general more discriminating branches were found corresponding to head shape or facial features.

Facial features in the OASIS dataset have been reduced to prevent identification of any participants in the study [6]. However, it appears enough features remain to identify gender of the participants. This is not a violation of the participant's privacy, because gender is a labeled attribute in the set, and thus determining it adds no information which was not already known. However, it is interesting that even the reduced facial features proved useful for distinguishing the gender of participants.

Our accuracy in gender determination is not as high as existing results automatically classifying gender based on pictures of the face. As a comparison, Baluja et al. obtained 90% accuracy determining gender from a 20*20 pixel grayscale image [20]. However, that our program is taking into account facial features is simply an unintended consequence of allowing the entire MR image to be evaluated by the program, rather than an intended result of the experiment.

Other findings such as [21] also show gender-based cranial differences. In [21], Gur et al. measure factors such as total gray matter volume, total white matter volume, CSF volume, and head size. Significant gender-based differences are found. Because the system does not distinguish between white and gray matter, it cannot discover some of these differences at this time.

We are aware of no existing system that automatically classifies MR images based on gender, whether using facial features, head shape, or brain structure.

D. Socioeconomic status

Hackman et al. noted cognitive and electrical activity correlations with socioeconomic status [22]. Socioeconomic status is an attribute in the OASIS dataset. Unfortunately, the system proved unable to distinguish between individuals with maximal and minimal socioeconomic status. This does not preclude a structural correlation with socioeconomic status, only indicates that one cannot be found as easily as correlations with gender, education, aging, and Alzheimer's disease.

VIII. FUTURE WORK

At present, our program does not incorporate gray vs. white matter distinction. Adding this capability may increase correlations which can be discovered. In particular, it may enable automatic discovery of gender-based characteristics as identified in [21].

The current work is intended as a component of a larger system which would more completely represent the brain in graph form. Currently, at least two approaches exist to forming a graph of connected neural components. Eguíluz et al. use functional MRI activation levels in order to link areas of the

brain with correlated activation in [23]. This produces a graph where two nodes are linked if the areas they represent activate at the same times. This is considered to be a functional brain network [24]. A different approach is taken by Hagmann et al. in [25]. A graph is formed of the structure of the brain, indicating which neural component is connected to which other neural component by analysis of white matter. This forms a structural brain network [24].

Trees as used in this paper may be incorporated into a network representing neural connections, to add information about physical properties of each neural component to the graph. A discriminating subgraph found in such a graph could include details of the shape of several components, and potentially discover correlations involving a number of items which are not obviously related.

IX. Conclusion

This work was intended to explore the utility of representing the shape of the entire brain using a graph, and the ability of frequent subgraph mining to discover discriminating pieces of the graph. The system was able to successfully classify individuals based on gender, age, level of education, and degree of cognitive impairment due to Alzheimer's disease. This demonstrates the versatility of the method. We are aware of no previous work on automatically determining gender based on MR images. We also provided a branch selection method similar to cross-validation which finds branches in the training set, and evaluates branches in the test set by how consistently each branch is discovered. Branches evaluated in this manner can be used to highlight areas the program has found useful for classification, which may be used to find correlations between brain structure and function or life events.

References

[1] E. Maguire, H. Spiers, C. Good, T. Hartley, R. Frackowiak, and N. Burgess, "Navigation expertise and the human hippocampus: a structural brain imaging analysis," *Hippocampus*, vol. 13, no. 2, pp. 250–259, 2003.

[2] A. Elsayed, F. Coenen, C. Jiang, M. García-Fiñana, and V. Sluming, "Corpus callosum MR image classification," *Knowledge-Based Systems*, vol. 23, no. 4, pp. 330–336, 2010.

[3] C. Nosarti, M. Al-Asady, S. Frangou, A. Stewart, L. Rifkin, and R. Murray, "Adolescents who were born very preterm have decreased brain volumes," *Brain*, vol. 125, no. 7, pp. 1616–1623, 2002.

[4] A. Du, N. Schuff, D. Amend, M. Laakso, Y. Hsu, W. Jagust, K. Yaffe, J. Kramer, B. Reed, D. Norman *et al.*, "Magnetic resonance imaging of the entorhinal cortex and hippocampus in mild cognitive impairment and alzheimer's disease," *Journal of Neurology, Neurosurgery & Psychiatry*, vol. 71, no. 4, p. 441, 2001.

[5] S. Nestor, R. Rupsingh, M. Borrie, M. Smith, V. Accomazzi, J. Wells, J. Fogarty, and R. Bartha, "Ventricular enlargement as a possible measure of alzheimer's disease progression validated using the alzheimer's disease neuroimaging initiative database," *Brain*, vol. 131, no. 9, p. 2443, 2008.

[6] D. Marcus, T. Wang, J. Parker, J. Csernansky, J. Morris, and R. Buckner, "Open Access Series of Imaging Studies (OASIS): cross-sectional MRI data in young, middle aged, nondemented, and demented older adults," *Journal of Cognitive Neuroscience*, vol. 19, no. 9, pp. 1498–1507, 2007.

[7] D. J. Cook and L. B. Holder, "Graph-based data mining," *IEEE Intelligent Systems*, vol. 15, no. 2, pp. 32–41, 2000.

[8] S. Klöppel, C. Stonnington, C. Chu, B. Draganski, R. Scahill, J. Rohrer, N. Fox, C. Jack Jr, J. Ashburner, and R. Frackowiak, "Automatic classification of mr scans in alzheimer's disease," *Brain*, vol. 131, no. 3, pp. 681–689, 2008.

[9] R. Cuingnet, E. Gerardin, J. Tessieras, G. Auzias, S. Lehéricy, and M. Habert, "Automatic classification of patients with alzheimer's disease from structural mri: A comparison of ten methods using the adni database," *Neuroimage*, 2010.

[10] S. Long and L. Holder, "Graph-based shape analysis for mri classification," *International Journal of Knowledge Discovery in Bioinformatics (IJKDB)*, vol. 2, no. 2, pp. 19–33, 2012.

[11] K. Millman and M. Brett, "Analysis of functional magnetic resonance imaging in Python," *Computing in Science & Engineering*, pp. 52–55, 2007.

[12] V. Megalooikonomou, J. Ford, L. Shen, F. Makedon, and A. Saykin, "Data mining in brain imaging," *Statistical Methods in Medical Research*, vol. 9, no. 4, p. 359, 2000.

[13] C.-C. Chang and C.-J. Lin, *LIBSVM: a library for support vector machines*, 2001, software available at http://www.csie.ntu.edu.tw/ cjlin/libsvm.

[14] R. Kohavi, "A study of cross-validation and bootstrap for accuracy estimation and model selection," in *International joint Conference on artificial intelligence*, vol. 14. LAWRENCE ERLBAUM ASSOCIATES LTD, 1995, pp. 1137–1145.

[15] D. Alley, K. Suthers, and E. Crimmins, "Education and cognitive decline in older americans," *Research on aging*, vol. 29, no. 1, p. 73, 2007.

[16] R. Wilson, Y. Li, N. Aggarwal, L. Barnes, J. McCann, D. Gilley, and D. Evans, "Education and the course of cognitive decline in alzheimer disease," *Neurology*, vol. 63, no. 7, p. 1198, 2004.

[17] C. Coffey, J. Saxton, G. Ratcliff, R. Bryan, and J. Lucke, "Relation of education to brain size in normal aging," *Neurology*, vol. 53, no. 1, pp. 189–189, 1999.

[18] J. Goldstein, L. Seidman, N. Horton, N. Makris, D. Kennedy, V. Caviness, S. Faraone, and M. Tsuang, "Normal sexual dimorphism of the adult human brain assessed in vivo magnetic resonance imaging," *Cerebral Cortex*, vol. 11, no. 6, p. 490, 2001.

[19] R. Lenroot, N. Gogtay, D. Greenstein, E. Wells, G. Wallace, L. Clasen, J. Blumenthal, J. Lerch, A. Zijdenbos, A. Evans *et al.*, "Sexual dimorphism of brain developmental trajectories during childhood and adolescence," *Neuroimage*, vol. 36, no. 4, pp. 1065–1073, 2007.

[20] S. Baluja and H. Rowley, "Boosting sex identification performance," *International Journal of Computer Vision*, vol. 71, no. 1, pp. 111–119, 2007.

[21] R. Gur, B. Turetsky, M. Matsui, M. Yan, W. Bilker, P. Hughett, and R. Gur, "Sex differences in brain gray and white matter in healthy young adults: correlations with cognitive performance," *The Journal of Neuroscience*, vol. 19, no. 10, pp. 4065–4072, 1999.

[22] D. Hackman and M. Farah, "Socioeconomic status and the developing brain," *Trends in Cognitive Sciences*, vol. 13, no. 2, pp. 65–73, 2009.

[23] V. Eguiluz, D. Chialvo, G. Cecchi, M. Baliki, and A. Apkarian, "Scale-free brain functional networks," *Physical Review Letters*, vol. 94, no. 1, p. 18102, 2005.

[24] E. Bullmore and O. Sporns, "Complex brain networks: graph theoretical analysis of structural and functional systems," *Nature Reviews Neuroscience*, vol. 10, no. 3, pp. 186–198, 2009.

[25] P. Hagmann, M. Kurant, X. Gigandet, P. Thiran, V. Wedeen, R. Meuli, and J. Thiran, "Mapping human whole-brain structural networks with diffusion MRI," *PLoS One*, vol. 2, no. 7, p. 597, 2007.